International Journal of Mechanical, Industrial and Aerospace Sciences
ISSN: 2517-9950
Vol:8, No:11, 2014

Studies of Interfacial Microstructure and Mechanical Properties on Dissimilar Sheet Metal Combination Joints Using Laser Beam Welding

K. Kalaiselvan, A. Elango

Abstract**—**Laser beam welding of dissimilar sheet metal combinations such as Ti/Al, SS/Al and Cu/Al are increasingly demanded due to high energy densities with less fusion and heat affected zones. A good weld joint strength involves combinations of dissimilar metals and the formation of solid solution in the weld pool. Many metal pairs suffer from significant intermetallic phase formation during welding which greatly reduces their strength. The three different sheet metal mentioned above is critically reviewed and phase diagram for the combinations are given. The aim of this study is to develop an efficient metal combinations and the influence on their interfacial characteristics. For that the following parameters such as weld geometry, residual distortion, micro hardness, microstructure and mechanical properties are analyzed systematically.

Keywords**—**Laser Beam Welding (LBW), dissimilar metals, Ti/Al, SS/Al and Cu/Al sheets.

I. Introduction

DEVELOPMENT of aircraft industry has been driven towards weight reduction and as a consequence, fuel consumption reduction due to tightening of ecological and economical constraints. Customized materials combine with high stiffness, corrosion resistance and strength. Joining of dissimilar is often demanding. Laser processing offers an advantage since thermal input is minimized due to the well localized spot size and high processing speed. Joining Titanium and Aluminum alloys could be advantages compared to conventional methods [1]. At different laser centers [1]-[3] an increased amount of hybrid Ti/Al structure welding are in progress.

Joining titanium to aluminum is the formation of intermetallic phases, which depends on process, related temperature-time cycles [4], [5]. These cycles are obviously associated with non-equilibrium metallurgical phenomena and the equilibrium phase diagram of titanium and aluminium is to be considered. The binary Ti–Al phase diagram [6] is shown in Fig. 1. It shows the phase formation behavior. On the titanium-rich side, a slightly lower solubility for aluminum is clear. Exceeding aluminum content of approximately 13% in the titanium results in Ti_3Al formation. With increasing aluminum content, phases like Ti, Al and then $TiAl_2$ are formed. On the aluminum rich side of the diagram, the low solubility of titanium leads to early formation of the intermetallic phase $TiAl_3$ when the titanium content exceeds approximately 2 at%. Based on thermodynamic assumptions, it is predicted that in the first stage during the reaction of titanium and aluminum, the $TiAl_3$ phase forms preferentially [7] and this phase induces joint embrittlement. However, if metal joints with high toughness and strength are required, the intermetallic phase layer has to be limited to a maximum thickness of less than 10 mm [8].

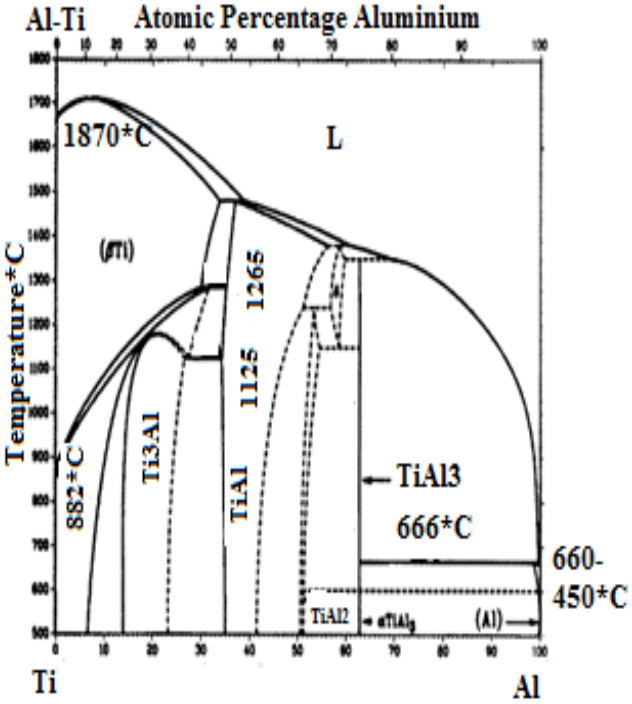

Fig. 1 Binary Ti–Al equilibrium phase diagram

Fig. 2 shows the dual phase diagram of Fe-Al. Thermal joining methods like arc or laser welding suffer from the formation of brittle intermetallic compounds. Joining of aluminum with other materials used in car body manufacturing is often challenging. The amount of steel used in car body manufacturing has decreased continuously and aluminum content increases for weight reduction. 1 kg aluminum substituting a heavier automotive component helps to avoid 20 kg green house gas during operating life [9].

K.Kalaiselvan is with the Anna University Affliated Engineering College, Tamilnadu – 630004 (Cell No. 8891491686; e-mail:kalaiesanai@gmail.com).
Dr.A.Elango is a Vice Principal with the Anna University Engineering College, Tamilnadu – 630004 (e-mail:elango.arum69@gmail.com).

Passenger safety and comfort demands have increased average vehicle weight in the compact class by almost 50% during the last 40 years [10].

In the atomic scale the atoms of the aluminum alloys and steels can be moved during the bonding processes as a function of the number of vacancies, diffusion of small solute like carbon and hydrogen which is called interstitial diffusion and grain boundary moving. The equilibrium phase diagram shows [11] seven non-stoichiometric intermetallics: Fe_3Al, FeAl ($\alpha 2$), $FeAl_2$, Fe_2Al_3 (ε), Fe_2Al_5, $FeAl_3$ and $FeAl_6$.

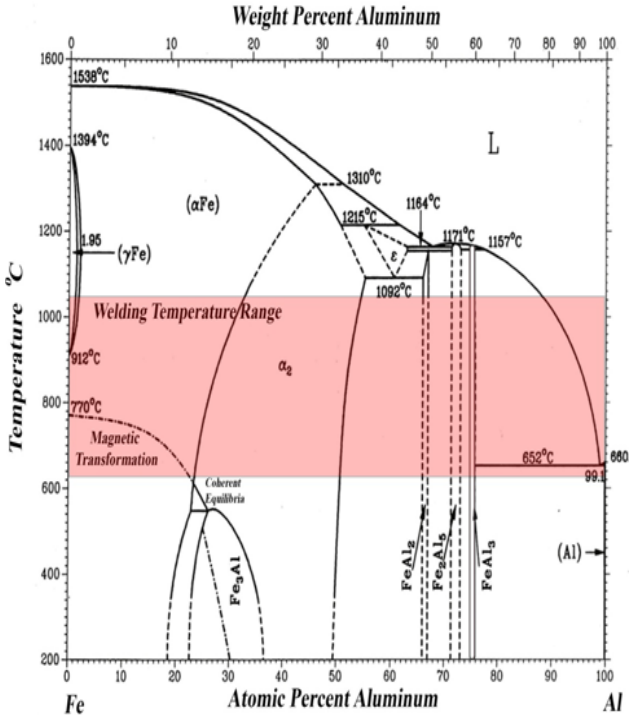

Fig. 2 The dual phase diagram of Fe-Al

Cu/Al combination finds particular use in electrical and electronic applications. Aluminium has high electrical conductivity, reflectivity and corrosion resistance. Many research efforts have been made in the area of laser beam welding. Copper-Aluminium binary phase diagram [12] is shown in Fig. 3.

Binary aluminium bronzes are classified in to non-heat treatable α aluminium bronzes containing between 5 and 8% Al and complex, heat treatable aluminium bronzes containing more than 8% Al. A martensitic transformation is possible only in alloys richer in 8% Aluminium. The type of martensite is dependent on aluminium content. Between 8 and 11% Al an ordering reaction prior to the formation of martensite does not occur and the formation of martensite is denoted (β). Between 11 and 13 wt% Al, ordering to β_1 occurs before the martensite transformation and an ordered martensite (β') forms. In alloys containing between 13 and 15 wt% Al, the β_1 structue decomposes to γ', an internally twinned orthorhombic martensite. On slow cooling the development of microstructures in complex aluminium bronze occurs by eutectoid reaction which produces an α plus γ_2 coupled eutectoid structure which gives poor mechanical and corrosion performance.

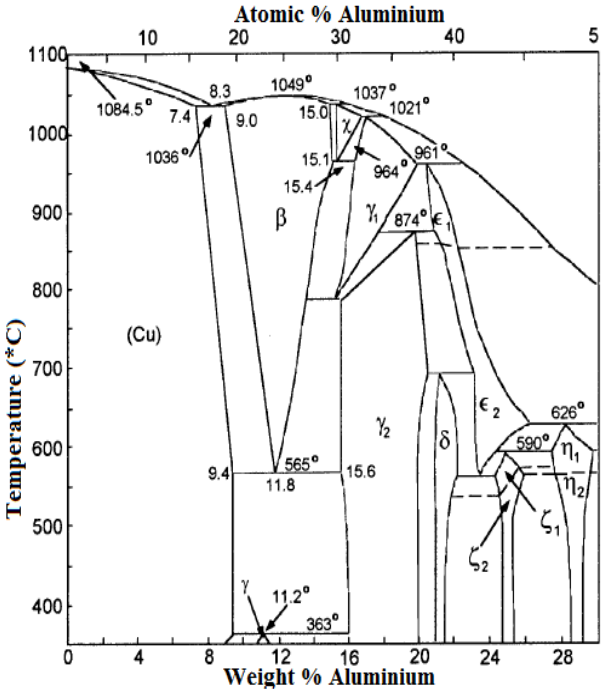

Fig. 3 Binary - Copper Aluminium phase diagram

II. Literature Discussion

A. Titanium/Aluminium Joint

Joining Ti/Al alloys thin sheet is of interest to meet the requirement of high strength and low weight in aeronautic and automotive industries. Zhihua Song et al. [13] discussed the direct welding of Ti6Al4V/A6061 dissimilar alloys with 2mm thickness by laser beam without filler metal which can produce sound brazing joints with good appearance under welding conditions of 4kW laser power, 4m/min welding speed and 0.8–1.0mm laser offset at aluminum alloy side. Laser offset has a great influence on the thickness of interfacial intermetallic compound (IMC) layer and the mechanical property of joint.

Fig. 4 shows interfacial microstructures by Optical micrographs (OM) and scanning electron microscope (SEM) at the top of joint with various laser offsets. When the laser offset is 0.7 mm, the interfacial IMC layer has thick continuous morphology and discontinuous cub shaped morphology. The interfacial IMC layer is identified as TiAl3 by energy dispersive x-ray spectroscopy (EDX). Offset is increased to 0.8mm, the IMC layer exhibits a continuous morphology and 0.9–1.0mm a discontinuous serrate shape.

Fig. 5 presents the average thickness of interfacial IMC layer offset in the range of 0.8–1.0mm and the interfacial IMC layer thickness decreases with increasing laser offset. Thickness of

interfacial IMC layer is about 0.26mm and the average tensile strength of joint is 64% of the aluminum alloy base metal.

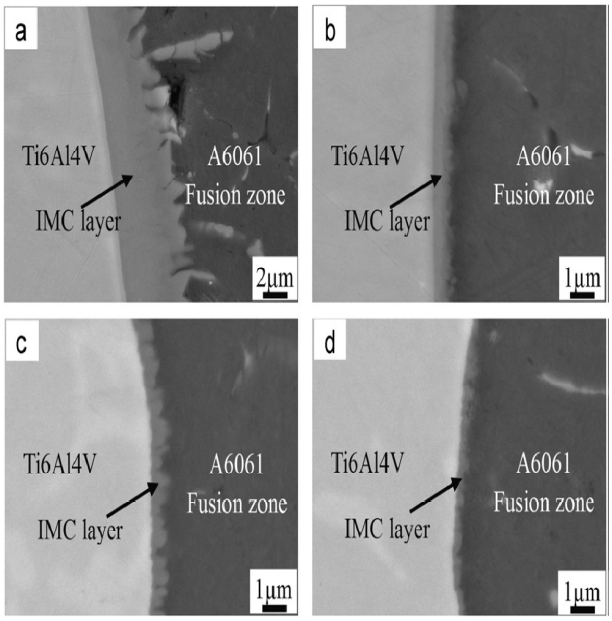

Fig. 4 Interfacial microstructures at top zone of Ti/Al joints with various laser offsets, (a) 0.7mm, (b) 0.8mm, (c) 0.9mm and (d)1.0mm

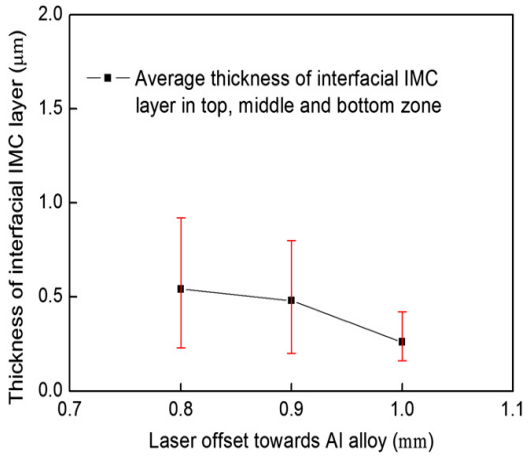

Fig. 5 Thickness of interfacial IMC layer with various laser offsets

Ming Gao et al. [14] developed dissimilar Ti/Al alloys in butt configuration using fiber laser cold metal transfer arc hybrid welding. Microstructure, interface properties, tensile behavior and their relationships are reported in detail.

Zhang et al. [15] shows cross-weld tensile strength is up to 213MPa and 95.5% that of laser cold metal transfer (CMT) welded 2mm thick AA6061 is 223MPa. Fig. 6 (a) shows that the strengths are above 200MPa when laser power is at the range of 2.0–2.5 kW, but decrease rapidly when laser power deviates from this range. Fig. 6 (b) shows the strengths are higher than 200MPa when wire filling rate corresponding to arc current increases to 5.4 m.min^{-1}. This indicates that tensile strength is more sensitive to laser power.

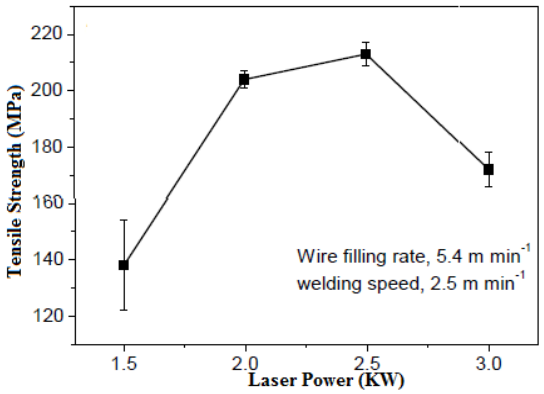

(a) Laser power

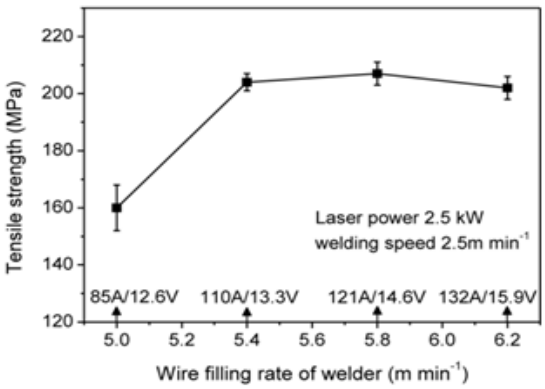

(b) Wire filling rate

Fig. 6 Tensile strength as a function of (a) laser power and (b) wire filling rate

The optimal range of heat input for accepted joints is obtained as 83–98 J·mm^{-1}. Within this range the joint is stronger than 200MPa and fractures at the intermetallic compounds (IMCs) layer which is about 1μm thick and consists of $TiAl_2$ due to fast solidification rate. This layer consists of a wide $TiAl_3$ layer close to FZ (Fusion Zone) and a thin $TiAl_2$ layer close to Ti substrate.

Möller et al. [16] show that the heat conduction in welding process is a feasible process for joining aluminium and titanium hybrid structures. It is demonstrated that the deformation prior to welding influences the deformation after welding. The thermo mechanical simulation gives distortion and residual stresses of the specimens after welding and the height distortion is caused by an occurring longitudinal plastic compression zone in the titanium component part. This plastic zone extends total length of the specimen and is created by the presence of a large direction specific resistance to the large local thermal expansion.

Vaidya et al. [17] reported that the grain size in the fusion zone is reduced and the intermetallic phase formed at the interface is thinner. Specimens could be mechanically tested

without formation of cracks in the reaction zone. It is found that the welded coupons are sound in both configurations. Hardness and tensile strength are slightly higher in the modified joint and the fracture occurred in the hardness dip on the side of AA6056–T6 and the interface remained intact in both cases. From the optical image analysis deformation is found to build up at about 7mm from the interface on the Al side. This is the hardness dip which being the weakest site in both joints it became liable for deformation and strain concentration is shown in Figs. 7 (a) and (b). The zone Al side alone exhibited high strain in both cases 15%. The interface itself had a higher strength and did not undergo deformation in the tensile test.

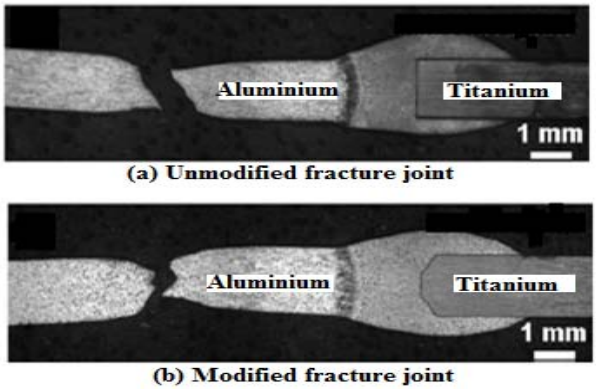

Fig. 7 Optical images of the fracture location (a) Unmodified joint and (b) Modified joint

During fatigue crack propagation partly intercrystalline fracture occurred in the fusion zone of the unmodified joint specimens. This is absent in the modified joint specimens and completely transcrystalline fracture also striations are observed. Decrease in the interfacial area the modified configuration is inferred to have induced a faster cooling rate. This has most likely decreased the reaction zone, improved the interfacial binding, reduced the grain size in the fusion zone, avoided grain boundary segregation and retained solute for hardening.

Shuhai Chen et al. [18] developed joining mechanism of Ti/Al dissimilar alloys using laser welding brazing process with automated wire feed. The microstructures of fusion welding and brazing zones are analyzed in details by transmission electron microscope (TEM). It is found that microstructures of fusion welding zone consist of α-Al grains and ternary near eutectic structure with α-Al, Si and Mg_2Si. Interfacial reaction layers of brazing joint are composed of α-Ti, nanosize granular $Ti_7Al_5Si_{12}$ and serration shaped $TiAl_3$. Apparent stacking fault structure in intermetallic phase $TiAl_3$ is found when the thickness of the reaction layer is very thin approximately less than 1μm.

Gerhard LIEDL et al. [19] laser assisted joining of dissimilar materials gives excellent results if parameters are adjusted carefully. Titanium and aluminum have been welded by means of a 3kW Nd:YAG laser with resulting very uniform and homogenous IMPs with a thickness of less than 10μm..

Michael Kreimeyer et al. [20] investigated the mechanical behavior of titanium-aluminum butt joint geometry and tensile testing. The joints are welded with laser beam power of 4.5kW and a joining speed of 100 mm/s. The tensile strength test comparison with the base material is presented in Fig. 8.

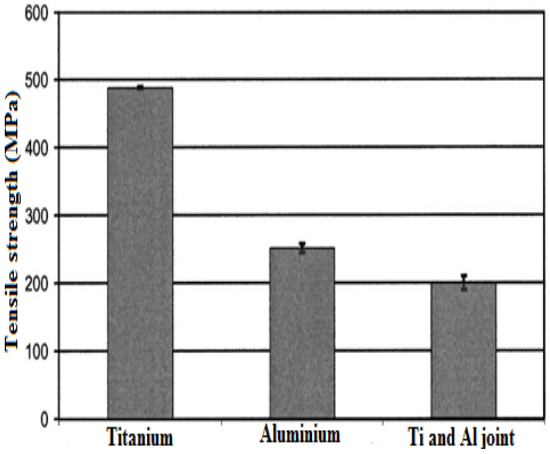

Fig. 8 Tensile strength of the titanium-aluminum butt joint in comparison with the base materials

The titanium reaches an average tensile strength of about 490MPa and the aluminum base material 250MPa. The titanium aluminum butt joint gives an average tensile strength of 200MPa which equals 80% of the strength of the aluminum base material.

B. Stainless Steel/Aluminum joint

Laser welding can be used to join steel and aluminum without the use of filler metal and low penetration depth increase in tensile strength. According to Schimek et al. [21] the joining mechanism between the steel and aluminum sheet the reduction of intermetallic brittle compounds is challenge in joining. A high welding depth increase mixing of iron, aluminum and of crack initiation. Lower welding depth in the cross-section between the steel and aluminum are insufficient for high strength welds. A small mixing of iron and aluminum implies high tensile shear strength of steel and aluminum. A formation of intermetallic phases results in high hardness and low deformation capacity.

Weld seams and force flow of steel and aluminum dissimilar compounds are shown in Figs. 9 (a) and (b) which are produced with a focus diameter of 1200μm and can increase maximum forces than dissimilar compounds that are produced with a focus diameter of 600μm.

In consideration to the force flow, welding seams which are produced with a various focus diameter and different forces exist. Shear stresses that act parallel to the intermetallic phases are more favorable. The displayed force flow red lines run through the steel sheet over the weld seam in the aluminum sheet. The weak point of the intermetallic phases at the specimen is produced with a focus diameter of 600μm occurs approximately orthogonal to the force flow lines.

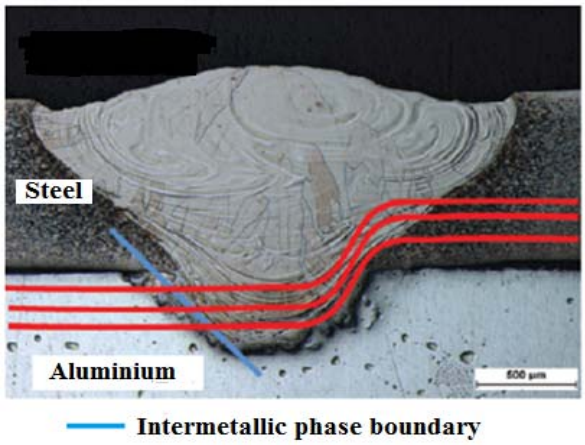

(a) Focus diameter of 1200µm

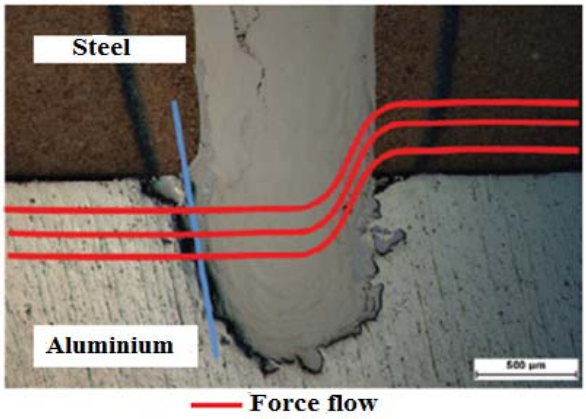

(b) Focus diameter of 600µm

Fig. 9 Weld seams and force flow of steel on aluminum hybrid structures produced with a focus diameter (a) of 1200 µm and (b) of 600 µm

Zhang et al. [22] carried automotive galvanized steel to aluminum alloy using fiber laser keyhole welding brazing technique. The microstructure characteristics and mechanical properties of the butt joint are investigated. A typical keyhole welded seam formed on the aluminum alloy side and a brazed seam generated on the solid galvanized steel side by fiber laser keyhole welding brazing technique without any shaped grooves. The dendritic eutectic structure and a great quantity of equiaxed crystal are formed at the center of welded seam. The columnar crystal is generated nearly vertical to the interfacial layer between galvanized steel and brazed seam. The thickness of the interfacial reaction layer is varied with joint zone ranged from 1.5 µm to 13 µm and composed of three different phases such as α (τ_5) - Al_8Fe_2Si, θ-$Al_{13}Fe_4$ and ζ-Al_2Fe with micro hardness ranging from ~811 HV to ~1060 HV.

The tensile strength of the laser keyhole welding brazed steel and aluminum hybrid joint is evaluated and is shown in Figs. 10 (a)-(c). It shows that three failure modes of joints are observed with different laser powers of 2300W, 2500W and 2600W also keeping other parameters is constant.

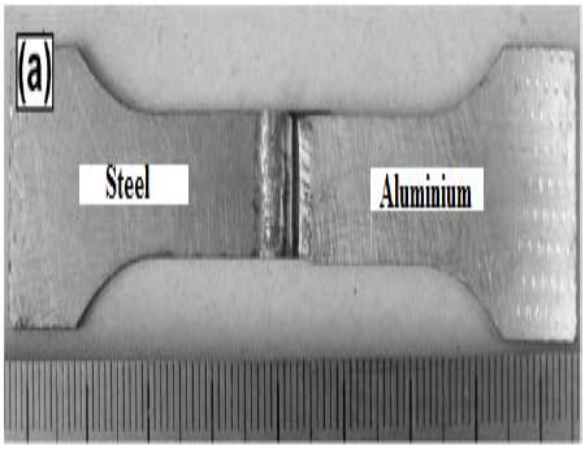

(a) Fractured at HAZ of aluminum alloy

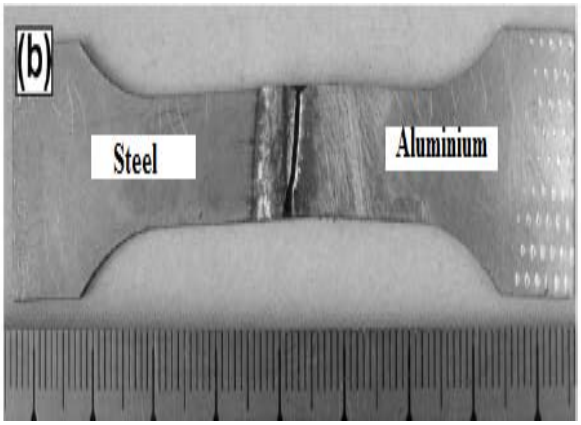

(b) Mix-failed through HAZ of aluminum alloy and brazed seam

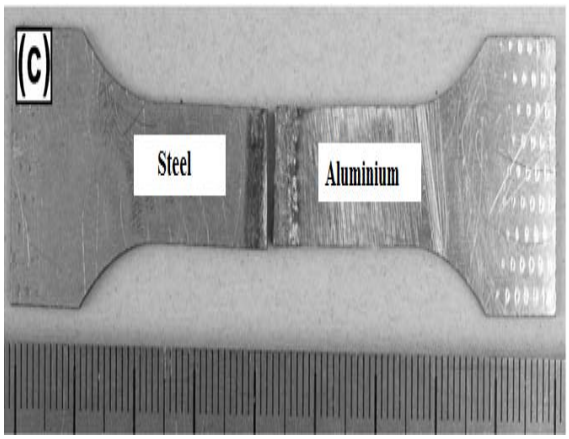

(c) Detached between galvanized steel and brazed seam

Fig. 10 Macroscopic view of failure specimens (a) Fractured at HAZ of aluminum alloy, (b) Mix-failed through HAZ of aluminum alloy and brazed seam and (c) Detached between steel and brazed seam

The best one is fractured at heat affected zone (HAZ) of aluminum alloy with appearance of necking in tension, as shown in Fig. 10 (a). The average tensile strength is up to 162MPa. The specimens are fractured through HAZ of aluminum alloy and welded seam simultaneously with average tensile strength of 140.5MPa as shown in Fig. 10 (b). The worst is detached between galvanized steel and brazed seam with average tensile strength of 124MPa as shown in Fig. 10 (c). This implies that the joint formed in higher heat input have a lower tensile strength than in lower heat input due to thicker intermetallic compound layer.

Kouadri-David et al. [23] have shown that the use of laser welding in the capillary vapour keyhole mode with galvanized sheet steel can result in joint shear strengths of 190MPa. Compared to the base metal, the welded joint shear strength obtained correspond to 60% that of aluminium and 30% that of DP600 steel. It is observed that the shear strength of LBW joint with 140Mpa is much lower than parent metal aluminium with 315Mpa and steel with 654Mpa. The advantage of this mode is the possibility to reduce the temperature gradient. This leads to a formation of a weld by two methods by forming a weld between the zinc and aluminium and by diffusion between the aluminium and the iron. The inconvenience of this mode is the need to produce a reaction layer of uniform thickness. The use of an alloy with a dense zinc layer is expected to increase the mechanical strength of these joints.

Thomy et al. [24] investigated the effect of process parameters on joint properties in laser MIG hybrid welding of aluminium to steel in butt joint configuration and a process parameter envelope is established. Within this parameter envelope, joints with optimized properties especially tensile strength exceeds 180MPa whereas, corrosion behavior of coated specimens produced within this envelope is rated not appreciable.

Theron et al. [25] discussed the possible operating windows for the SS/Al dissimilar metal combinations with the specific set up ranges between 0.75KW - 1.8KW and speed 1-7m/min. A 10 to 20% increase in welding power at constant travel speed resulted in a 40 to 65% increase in tensile strength for different spot sizes as shown in Fig. 11. Little scatter is noted for 0.3mm spot which is the optimum for SS/Al welding.

Jandaghi et al. [26] have developed the alloying elements which are controlled in weld metal by changing the laser parameters. Several experiments are performed and a theoretical model is developed for the determination of significant alloying element losses such as Mn, Cr, Ni, Mn, Al and Fe in the keyhole welding of SS-316 and Al5754 using a long pulsed Nd:YAG laser. Based on LIBS and WDX/EDX analysis and modeling Mn and Cr concentrations reduce within the weld metal where as Fe and Ni increase. It is found that Mg loss linearly increases with increasing the pulse duration of the laser welding and the variation of Mg trace is negligible while varying the laser power density.

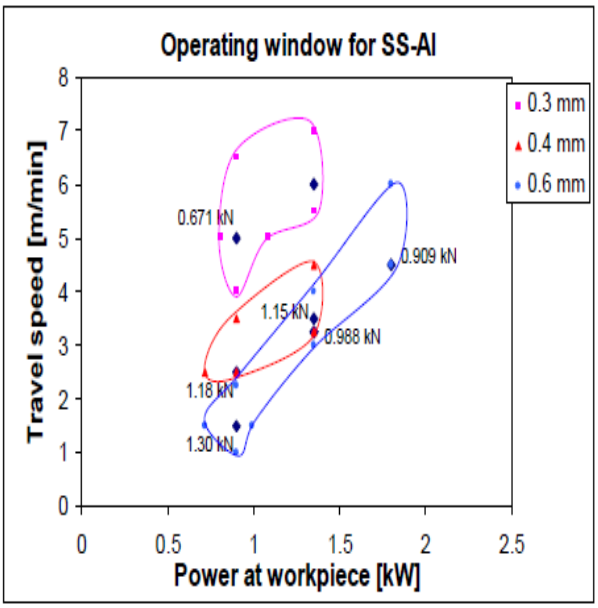

Fig. 11 Operating windows for SS/Al at the different spot sizes

C. Copper/Aluminium Joint

Cu/Al combination finds particular use in electrical and electronic applications. Aluminium has high electrical conductivity, reflectivity and corrosion resistance.

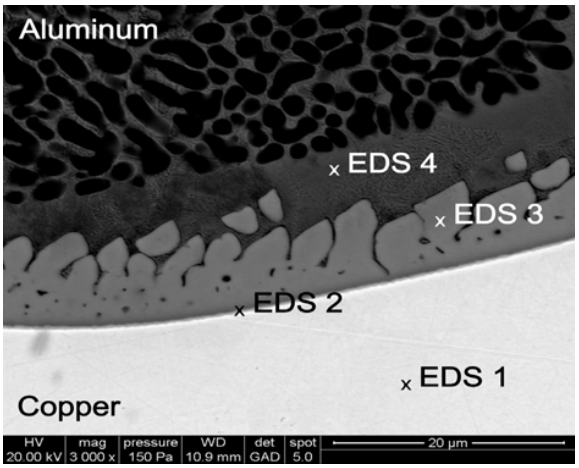

Fig. 12 IMC seam formation after laser beam braze welding

Compared to copper it is slightly lower thermal and electrical conductivity. Tobias Solchenbach et al. [27] found that low contact resistance is achieved by laser braze welding of Cu/Al joints. Also Intermetallic compounds had a strong impact on the contact resistance above thickness of 3–5µm and a thickness of 3.2µm has been observed for good welds. EDS analysis in Fig. 12 shows IMC seam formation after laser beam braze welding.

The marker EDS1 represents the copper bulk material. Traces of Al may be wiped over the Cu layer. EDS2 occurred near the copper rich compound layer. Near to the aluminum layer an aluminum rich compound EDS3 is observed and it

indicates the growth direction during the braze welding process from copper to aluminum. The Al rich compound is several times thicker than the Cu rich one. EDS4 represents a phase with eutectic structure between the Al bulk material and the Al rich intermetallic compound. The EDS results imply the growing amount of aluminum from EDS 2 to EDS 4. The lamellar shaped phase EDS4 is consistent with the composition at the Al rich eutectic point at 548◦C [28]. Lowest contact resistance and higher mechanical interface strength are achieved with the same process parameters and contact resistance is less sensitive to the intermetallic thickness than the mechanical strength.

Xiao Wang et al. [29] described an advanced technique for metal welding and composite production of laser shock welding. Experiments are conducted to verify the welding ability of aluminum/aluminum and aluminium/copper plates. Two kinds of interface morphologies are observed by metallographic investigation on cross sections of the joint areas including the linear and wavy interfaces. Micro hardness testing results show the welded interface has a much greater hardness than the base metals. The average Vickers micro hardness (HV) values measured in the interface region are shown in Fig. 13. Welding dissimilar metal couples it can be found that the hardness of measured zone increases as the distance from the interface of samples decreases.

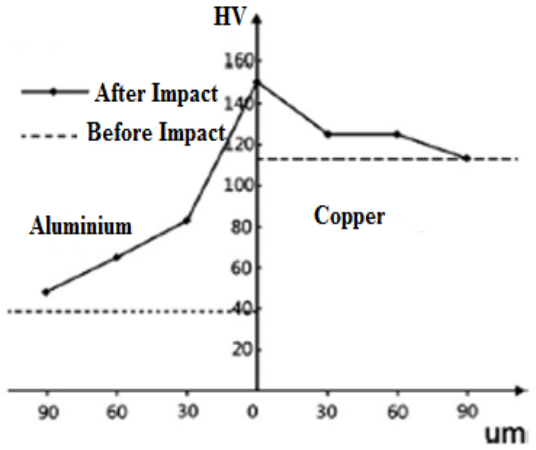

Fig. 13 Micro hardness in welding zone of Al/Cu

Tobias Solchenbach et al. [30] developed a novel laser braze welding process for dissimilar Al/Cu connections where the lower melting aluminum layer is melted and wets the copper surface. The Cu layer stays in solid state during the complete process. Detailed analysis of different response values with the help of a central composite design of experiments a processing window and the effect of the overlap, amplitude and laser power is identified. Intermetallic seam structure is shown in Fig. 14 that, over welding of the interface provides a better mechanical performance than under welding and higher shear strength of 121MPa.

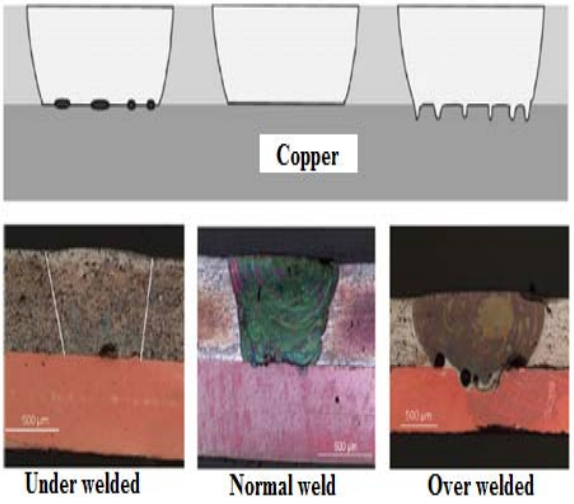

Fig. 14 Intermetallic seam structures

Theron et al. [25] reported Cu/Al operating windows for the specific setup ranges approximately between 1.2KW and 3.7KW at a travel speed between 2-8m/min. The higher tensile strength is obtained at the lower power levels and travel speeds. Least scatter is obtained with power densities between 17 and 26 KW/mm^2. Also 7-15% variations in power at constant travel speed and 35-50% variation in tensile shear strength for the different spot sizes are noted. The 0.4mm spot size is the optimum for Cu/Al welding.

Solchenbach et al. [31] investigated a combined laser beam braze welding process for flux less Al/Cu connections. A fibre laser in combination with a 2D scanner optic is used to enable superposed circular beam movements. By controlling the laser power and the geometrical overlap of a superposed circular beam movement, the optimal process parameters have been found experimentally. It is proved that the formation of intermetallic compounds is considerably reduced which leads to high shear strength up to 51MPa at the interface. The upper limit for intermetallic compounds at Al/Cu connections is measured to 4µm and the fracture of the specimen takes place at the Cu side.

III. Conclusion

In conclusion the study can be summarized as follows:

1. The formation of interfacial IMC layer, microstructure and its effect on the mechanical properties of the dissimilar Ti/Al, SS/Al and Cu/Al joint are discussed.
2. laser beam without filler metal can produce sound brazing joints with good appearance under welding conditions of 4kW laser power, 4m/min welding speed and 0.8–1.0mm laser offset at aluminum alloy side.
3. The titanium aluminum butt joint gives an average tensile strength of 200MPa which equals 80% of the strength of the aluminum base material.
4. The joining mechanism between the steel and aluminum sheet is similar to a tooth and challenge the reduction of intermetallic brittle compounds.

5. The steel and aluminium joint formed in higher heat input should have a lower tensile strength than in lower heat input because the brittle IMCs layer is thicker.
6. In welding of Cu/Al joint, the Intermetallic compounds had a strong impact on the contact resistance above a thickness of 3.5–5µm and a thickness of 3.2µm have been observed for good welds.
7. In Cu/Al joint, the micro hardness testing results show that welded interface has more hardness than the base metals.
8. Over welding of the interface provides a better mechanical performance than under welding of copper/aluminum.
9. For good weld joint, formation of solid solution in the weld pool is needed to minimize the thickness of intermetallic phase in fusion zone for dissimilar metal joints.

REFERENCES

[1] M. Kreimeyer. F. Wagner, and F. Vollertsen, Optics and Lasers in Engineering (2005).43, 9.
[2] E. Anawa., O. M. Elmabrouk, and A. Olabi, in IEEM 2009. IEEE "International Conference on Industrial Engineering and Engineering Management", (2009) in: edited by IEEE (IEEE, Piscataway, N.J).
[3] A. Saliger, Diploma thesis, Technische Universität, 2010.
[4] Sepold G., Schubert E, and Zerner I. "Laser beam joining of dissimilar materials", (1999). IIW-paper IV 734-99, Lisbon.
[5] Davis JR, "Aluminum and aluminum alloys",(1994). ASM International handbook. ASM International.
[6] Michael Kreimeyer, Florian Wagner, and Frank Vollertsen, "Laser processing of aluminum–titanium-tailored Blanks", (2005). Optics and Lasers in Engineering 43, 1021–1035.
[7] Wo¨hlert S, and Fru¨hstadien der Phasenbildung, "System Titan-Aluminium", (1995). Dissertation, Technische Universita¨ t Hamburg-Harburg.
[8] Lison R., Verbindungsschwei Xen unterschiedlicher, Werkstoffe—exemplarisch vorgestellt. In: Jahrbuch Schwei Xtechnik 99. Du¨ sseldorf. Herausgeber: DVS—Deutscher Verband fu¨ r Schwei Xen und verwandte Verfahren e.V; (1999). p. 35–48.
[9] International Aluminium Institute, "Improving Sustainability in the Transport Sector Through Weight Reduction and the Application of Aluminium", (2008). http://www.world-aluminium.org/ cache/ fl0000172.pdf.
[10] European Aluminum Association, "Aluminium in cars", (2008), http://www.eaa.net/upl/ 4/en/ doc/ Aluminium_in_cars..pdf.
[11] C.M. Wayman, "Introduction to the crystallography of Martensitic Transformations",(1964). Macmillan, New York.
[12] Hyatt, and Calvin V. 'Review of Literature Related to Microstructural Development During Laser Surface Engineering of Nickel Aluminium Bronze",(1997). Technical Memorandum, 31-59.
[13] Zhihua Song., KazuhiroNakata, AipingWu, and JinsunLiao, "Interfacial microstructure and mechanical property of Ti6Al4V/A6061 dissimilar joint by direct laser brazing without filler metal and groove", (2013). Materials Science & Engineering A 560 , 111–120.
[14] Ming Gao., Cong Chen., Yunze Gu, and Xiaoyan Zeng, "Microstructure and Tensile Behavior of Laser Arc Hybrid Welded Dissimilar Al and Ti Alloys", (2014). Materials, 7, 1590-1602.
[15] Zhang. C., Li. G, and Gao. M "Microstructure and process characterization of laser-cold metal transfer hybrid welding of AA6061 aluminum alloy", (2013). Int. J. Adv. Manuf. Technol, 68, 1253–1260.
[16] F. Möller*. M., Grden. C., Thomy, and F. Vollertsen, "Combined Laser Beam Welding and Brazing Process for Aluminium Titanium Hybrid Structures",(2011). Physics Procedia 12, 215–223.
[17] W. V. Vaidya., M. Horstmann., V. Ventzke., B. Petrovski., M. Koc¸ak., R. Kocik, and G. Tempus, "Improving interfacial properties of a laser beam welded dissimilar joint of aluminium AA6056 and titanium Ti6Al4V for aeronautical applications", (2010). J Mater Sci 45:6242–6254.
[18] Shuhai Chen., Liqun Li., Yanbin Chen, and Jihua Huang, "Joining mechanism of Ti/Al dissimilar alloys during laser welding-brazing process", (2011). Journal of Alloys and Compounds 509,891–898.
[19] Gerhard Liedl, Alexander Kratky, Matthias Mayr, and Alexandra Saliger, "Laser Assisted Joining of Dissimilar Materials",(2011). -ICF-Processing, Performance and Failure Analysis of Engineering Materials, 14-17 Nov. Luxor, Egypt.
[20] Michael Kreimeyer, Florian Wagner, and Frank Vollertsen, "Laser processing of aluminum–titanium-tailored blanks", (2005). Optics and Lasers in Engineering 43, 1021–1035.
[21] M. Schimek, A. Springer, S. Kaierle, D. Kracht, and V. Wesling, "Laser-welded dissimilar steel-aluminum seams for automotive lightweight construction",(2012). Physics Procedia 39, 43 – 50.
[22] M.J. Zhang., G.Y. Chen., Y. Zhang, and K.R. Wu, "Research on microstructure and mechanical properties of laser keyhole welding–brazing of automotive galvanized steel to aluminum alloy", (2013). Materials and Design 45, 24–30.
[23] A. Kouadri-David, and PSM Team, "Study of metallurgic and mechanical properties of laser welded heterogeneous joints between DP600 galvanised steel and aluminium 6082', (2014) Materials and Design 54 184–195.
[24] C Thomy, and F Vollertsen, "Laser -MIG Hybrid welding of aluminium to steel – Effect of process parameters on joint properties", (2009). XII-1958-09, BIAS Bremer Institut für angewandte Strahltechnik, Bremen, Germany.
[25] M.Theron., C.Van Rooyan, and L.H Ivanchev, "CW ND: YAG Laser welding of dissimilar sheet metals". Paper # 803, National laser center, CSIR, South Africa.
[26] M. Jandaghi., P. Parvin., M. J. Torkamany, and J. Sabbaghzadeh, "Alloying elemental change of SS-316 and Al-5754 during laser welding using real time laser induced breakdown spectroscopy (LIBS) accompanied by EDX and PIXE microanalysis", (2010). Physics Procedia 5, 107–114.
[27] Tobias Solchenbach, Peter Plapper, and Wayne Cai, 'Electrical performance of laser braze-welded aluminum–copper interconnects", (2014). Journal of Manufacturing Processes xxx , xxx–xxx.
[28] ASM handbook: volume 03, "alloy phase diagrams", (1992). ASM International.
[29] Xiao Wang., Chunxing Gu., Yuanyuan Zheng., Zongbao Shen, and Huixia Liu, "Laser shock welding of aluminum/aluminum and aluminum/copper plates", (2014). Materials and Design 56, 26–30.
[30] Tobias Solchenbach, and Peter Plapper, "Mechanical characteristics of laser braze-welded aluminium–copper connections", (2013) Optics & Laser Technology 54, 249–256.
[31] T. Solchenbach, P. Plapper, and "Combined Laser Beam Braze-Welding Process for Fluxless Al-Cu Connections", (2013). Laser Technology Competence Centre, Research Unit in Engineering Science, University of Luxembourg.